

## Effect of interface disorder on the confined phonon modes of GaAs/AlAs superlattices

D. Kechrakos, P. R. Briddon,\* and J. C. Inkson

Department of Physics, University of Exeter, Stocker Road, Exeter EX4 4QL, United Kingdom

(Received 17 May 1991)

We study the longitudinal optical-phonon modes in GaAs/AlAs(001) superlattices with disordered interfaces, using an 11-parameter rigid-ion model and the coherent-potential approximation. We show that, due to interface disorder, the frequencies of the confined modes deviate substantially from the bulk dispersion curve, the zone-center optical anisotropy is reduced, and the electrostatic interface modes show in the Raman spectrum. Our results are in good agreement with existing Raman measurements.

There has recently been a great deal of interest in the vibrational properties of layered materials. Improvements in growth techniques have made it possible to grow ultrathin superlattices (SL) in which quantum-mechanical confinement of phonon modes is clearly seen. In particular, the optical bands of GaAs and AlAs do not overlap, so in a superlattice formed from these materials the optical modes are well confined within the parent crystal slab. The frequencies of the confined longitudinal optical (LO) modes of a SL can therefore be attributed to a confinement wave vector and compared to the corresponding frequencies of the bulk semiconductor in the crystal Brillouin zone,<sup>1</sup> a procedure known as unfolding. It was anticipated that the measurement of the frequencies of these confined modes by high-resolution Raman techniques<sup>2</sup> would be an accurate method of extracting the phonon band structure of bulk semiconductors.

However, a series of experiments<sup>3,4</sup> has shown that the unfolding procedure leads to serious deviations from the bulk dispersion where the latter is known from neutron measurements. In particular, the frequencies of the low-order LO GaAs-like confined modes fall below the values expected from the bulk dispersion, while in contrast high-order modes fall substantially above the expected values. The frequency shifts are too large to be accounted for by electrostatic arguments<sup>5</sup> or a charge-transfer mechanism.<sup>6</sup> On the contrary, interface roughness, which naturally occurs due to the growth procedure (e.g., molecular-beam epitaxy), is believed<sup>3,4,6</sup> to be responsible for the observed trend. This may prove to be of great practical use as the sensitivity of the phonon modes to atomic scale disorder at the interfaces makes these modes an ideal tool for interface characterization.

An early study of the effect of interface roughness was based on a linear-chain model<sup>3</sup> with an alloy potential added at the interface sites. This potential was obtained from a bulk coherent-potential-approximation (CPA) calculation and, therefore, neglected superlattice effects. More recently<sup>6</sup> the same problem has been tackled using a direct diagonalization approach with a large supercell using coupling constants fitted to the results of *ab initio* calculations. Although the experimental trend of the confined modes has been satisfactorily reproduced, the enormous computational effort required reduces the versatility of the approach, limiting it to ultrathin samples.

Here we present results of a full CPA calculation of the

phonon modes in GaAs/AlAs(001) superlattices with disordered interfaces. This approach goes beyond previous calculations<sup>3</sup> in that the interface alloy layers are properly embedded into a superlattice environment. Superlattice effects, i.e., confinement and the presence of interface modes are therefore treated exactly. Because our approach requires a relatively minimal computational effort, since the calculation proceeds only in the interface defect space, thicker samples, as frequently used in experiments, and extended defects can be treated.

We model the interface roughness by a random cationic intermixing confined to one monolayer ( $\sim 2.86$  Å) on either side of the interface, a condition realized in most samples.<sup>3,4</sup> To describe the average properties of the interface alloy we use the CPA in its formulation as an iterative scheme.<sup>7</sup> The self-consistency is achieved in the usual way by demanding the alloy fluctuations at each disordered site to be equal to zero. The average Green function of the disordered SL is obtained from the Green function of the ideal SL and the alloy self-energy (mass correction) that acts simultaneously at all the disordered sites. In this way the dependence of the alloy potential on the number of disordered layers and their position in the supercell is properly taken into account. The resolution of our results is greatly improved ( $0.5$  cm<sup>-1</sup>) by an analytic continuation scheme<sup>8</sup> implemented at the end of the self-consistent cycle. Further details of our calculation will be published in a forthcoming paper.

The Raman response of the SL is calculated using the bond polarizability model.<sup>2</sup> Here we only consider LO modes as they have been most extensively studied experimentally. The cross-polarization response in the back-scattering geometry,  $z(xy)\bar{z}$ , neglecting the modulation of the atomic polarizabilities, can be cast in terms of the Green function of the system as

$$R_{xy}(\omega) \propto -\frac{2\omega}{\pi} \sum_{\kappa, \kappa'} (-1)^{\kappa-\kappa'} \text{Im} G_{\kappa\kappa'}^{zz}(\mathbf{q} \rightarrow \mathbf{0}; \omega) \quad (1)$$

where  $\kappa$  and  $\kappa'$  label the atoms in the superlattice unit cell (cations, odd; anions, even) and the zone center is approached along the SL axis. The parallel-polarization response,  $z(xx)\bar{z}$ , can be similarly cast in the form

$$R_{xx}(\omega) \propto -\frac{2\omega}{\pi} \sum_{i, i' \in \text{IF}} (-1)^{i-i'} \text{Im} G_{ii'}^{zz}(\mathbf{q} \rightarrow \mathbf{0}; \omega) \quad (2)$$

with the summation in this case over the interface (IF) As sites only (labeled  $i$  and  $i'$ ).<sup>2</sup> In Eq. (2) the response is proportional to the local polarizability modulation which is assumed to be unchanged by the presence of the interface alloy. It should be noted that Eq. (2) predicts the Raman intensity to increase with order of confinement, in contrast to the observed situation where the detailed form of the Fröhlich interaction reverses this trend. This however is not important for the present discussion where only the frequencies of the modes are considered. The symmetric LO confined modes couple to light in the  $z(xy)\bar{z}$  geometry, while the antisymmetric ones couple in the  $z(xx)\bar{z}$  geometry. Thus, Eqs. (1) and (2) together provide the frequencies of all the LO confined modes of the ideal and disordered systems.

We describe the lattice dynamics of the bulk semiconductors by an 11-parameter rigid-ion model.<sup>9</sup> The SL dynamical matrix is obtained from the dynamical matrix of the primitive unit cell using the method of Kanellis<sup>5</sup> and parameters fitted to the bulk GaAs phonon spectrum.<sup>9</sup> It is anticipated that this set of parameters will give an accurate description of the GaAs-like modes, but it would be less accurate for the AlAs-like modes. We therefore concentrate in what follows on the GaAs frequency range only.

In Fig. 1 we show the frequency of the first confined LO mode for various SL thicknesses and for the case of maximum interface disorder ( $\text{Ga}_{0.5}\text{Al}_{0.5}$ ). A downshift compared to the ideal SL is seen in all cases but the monolayer SL. The reason for this behavior is that in the case of extreme confinement ( $n=1$ ) the bulk GaAs LO phonon ( $290\text{ cm}^{-1}$ ) suffers a large downshift ( $39\text{ cm}^{-1}$ ), due to the large LO bandwidth, and ends up below the corresponding frequency of the 50%-50% alloy ( $\omega_{\text{alloy}}=276\text{ cm}^{-1}$ ).

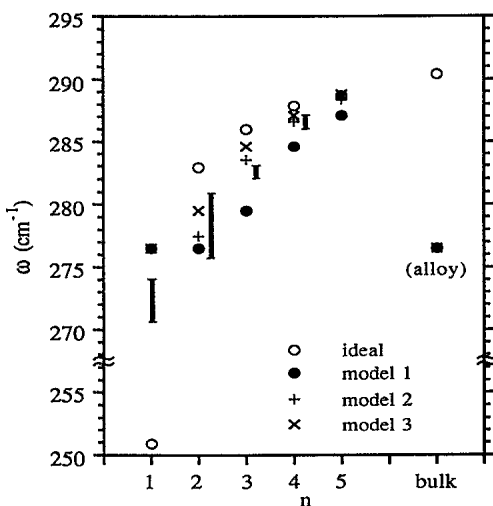


FIG. 1. Frequencies of the GaAs-like LO<sub>1</sub> modes. Model 1: Four disordered cationic planes in the supercell, two around each interface. Model 2: Two disordered cationic planes in the supercell, around one interface. Model 3: Two disordered cationic planes in the supercell, one on the same side of each interface. Alloy composition 50%-50% in all cases. Vertical bars equal experimental range from Ref. 4.

For systems thicker than one monolayer the possibility of only one interface being disordered occurs, which is a better model for the well-established asymmetric growth of GaAs/AlAs samples.<sup>10</sup> We see that this results in smaller shifts because the alloy-induced confinement is unilateral. For ultrathin samples ( $n \leq 4$ ) the shift is sensitive not only to the alloy content in the sample but also to the position of the random planes in the supercell; in particular, two alloy planes cause maximum downshift when they are next to each other (see Fig. 1), as in the asymmetric growth, because they form a wider barrier for the confined modes and are therefore highly impenetrable. The magnitude of the shift decreases with SL thickness as the interface region becomes a gradually smaller part of the supercell. The results for a 50%-50% alloy provide an upper limit to the shift of LO<sub>1</sub> due to interface disorder and in all cases the range of the measured frequencies<sup>4</sup> falls within our theoretical predictions; this allows us to have a first estimate of the amount of disorder of any particular sample by varying the alloy composition. More detailed characterization, however, requires the frequencies of higher order modes, which we now consider.

The results of the unfolding procedure are shown in Fig. 2 for the (5,5) and (10,10) SL and the Raman spectrum for the (5,5) SL is shown in Fig. 3. For the confinement wave vector of the  $s$ th mode in a system with  $n$  monolayers of the parent material we use the expression  $q_s = s\pi / [(n+0.5)a/2]$ .<sup>11</sup> The modes of the ideal SL fall quite accurately on the bulk dispersion, but the presence of interface disorder causes substantial deviations, which can be generally understood as follows: The  $\text{Ga}_{0.5}\text{Al}_{0.5}\text{As}$  alloy shows a two-mode behavior with the GaAs-like optical band falling between  $258$  and  $276\text{ cm}^{-1}$  within our model. The upper part of the GaAs LO band ( $k_z < 0.5$ ) lies well above the alloy band, and therefore confined modes originating from this part of the bulk band decay very fast in the alloy and are therefore confined to a narrower well which gives rise to a frequency downshift. Confined

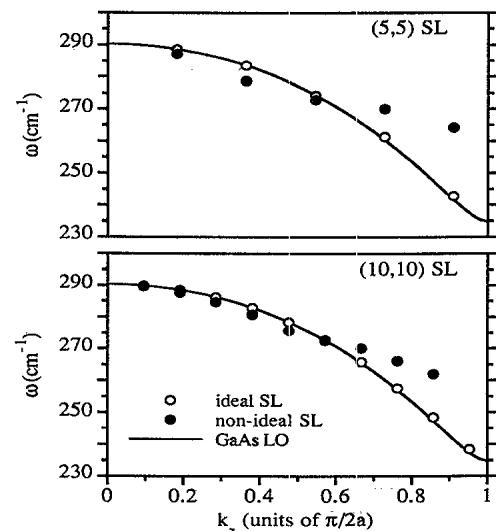


FIG. 2. Unfolding of the modes for (5,5) and (10,10) superlattices with two disordered planes at each interface (model 1). Alloy composition 50%-50%.

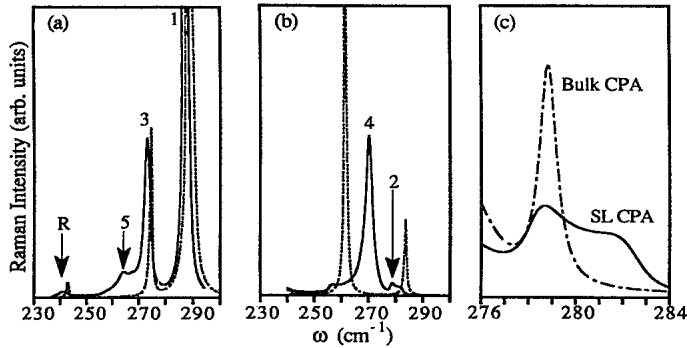


FIG. 3. Raman spectrum for the (5,5) SL with two disordered planes at each interface in (a)  $z(xy)\bar{z}$  and (b)  $z(xx)\bar{z}$  geometries. Dashed lines equal ideal SL; Full lines equal SL CPA; (c) part of (b) in the frequency range of the interface modes.

modes from the lower part of the GaAs LO band propagate in the alloy region and are therefore upshifted. The relatively broad linewidth of these modes (Fig. 3) is a manifestation of the strong alloy scattering. Notice that, for the (5,5) system, the  $LO_3$  mode lies within the alloy band and yet is still downshifted. This can be understood because, although the confinement length is increased, this is accompanied by an alloy mass at the interface that is heavier ( $\sim 25\%$ ) than the Ga mass. These two factors have opposite effects and, in this case, the heavier mass predominates. We can see that confined modes near the zone edge suffer the largest shifts and are therefore more suitable for interface characterization purposes. Finally, the experimental trend<sup>4</sup> is satisfactorily reproduced giving us confidence in our model and the description of the interface roughness.

Also we find [Fig. 3(a)] a peak in the Raman intensity of the (5,5) SL at a frequency close to the bottom of the bulk LO band ( $243\text{ cm}^{-1}$ ). Its frequency and projection on all the atomic planes (not shown here) are similar to those of the highest confined mode of the perfect SL that is seen in that geometry ( $LO_5$ ). A similar situation occurred for the (10,10) SL close to the ideal  $LO_9$  peak ( $\sim 248\text{ cm}^{-1}$ ). These peaks are in agreement with a recent experimental observation of a Raman line close to the bottom of the LO band with a frequency dependence on the SL thickness the same as that of the highest confined mode. We refer to this peak as the remnant (*R*) of the highest confined mode<sup>12</sup> and attribute it to the partial acoustic character of the GaAs-like confined modes originating from the bottom of the LO band.

It has been argued<sup>13</sup> that the relaxation of the  $\mathbf{q}=\mathbf{0}$  selection rule allows Raman scattering by interface modes of electrostatic origin. In Fig. 3(c), we compare the polarized Raman spectra obtained from a nonideal (5,5) system, using the self-energies obtained from the SL CPA and the CPA calculation for the bulk alloy. The latter treats the alloy effects only and neglects any effects due to the SL geometry, while the full SL CPA treats the alloy embedded in the SL and therefore allows for coupling be-

TABLE I. Frequencies in  $\text{cm}^{-1}$  of the principal GaAs-like modes in BS and FS geometries.

	(3,3) SL		(5,5) SL	
	Ideal	Nonideal	Ideal	Nonideal
BS	286.0	279.5	288.7	287.2
FS	274.9	273.5	279.0	280.5
Anisotropy	11.1	6.0	9.7	6.7

tween bulk-like (confined) and interface modes. The SL CPA spectrum shows a broad structure around  $280\text{ cm}^{-1}$ , which is the frequency range of the electrostatic interface modes within our model.<sup>11</sup> The absence of this feature in the bulk CPA calculation demonstrates that the peak observed experimentally<sup>13</sup> at this frequency is indeed due to scattering by the electrostatic interface modes, activated by interface roughness.

The zone-center-optical anisotropy<sup>11</sup> of the GaAs/AlAs SL can be deduced from the relative positions of the principal Raman peaks in the backscattering (BS) and forward scattering (FS) geometries.<sup>14</sup> In the forward scattering geometry, phonons propagating perpendicular to the SL axis are detected, and the infinitesimal wave vector in Eqs. (1) and (2) should therefore be parallel to the layers. We compare the frequencies of the principal lines in the depolarized Raman response for the two geometries in Table I. The interface disorder decreases the  $LO_1$  frequency in the BS geometry, as explained above, while it hardly shifts the principal peak in the FS. This behavior reflects the large dispersion of the  $LO_1$  mode arising from the long-range Coulomb forces. Increasing the proportion of disordered layers reduces the anisotropy (Table I). In the case of the (5,5) system with two alloy monolayers at each interface the  $LO_1$  peak is very close to the experimental value<sup>14</sup> ( $287\text{ cm}^{-1}$ ), but the calculated anisotropy ( $7\text{ cm}^{-1}$ ) remains larger than the measured value ( $4\text{ cm}^{-1}$ ). Since the modes showing in the FS geometry have a transverse polarization, this discrepancy could be due to polariton effects, but this point requires further investigation.

In summary, we have studied the off-resonance Raman spectrum of GaAs/AlAs SL with rough interfaces using a fully microscopic approach. We have shown that the inclusion of interface disorder bridges the gap between calculations of LO modes in ideal superlattices and Raman measurements. The observation of macroscopic interface modes and the reduction of the zone-center-optical anisotropy has been shown to result from the presence of interface roughness. Our results also demonstrate that an accurate lattice dynamics model combined with the CPA provide a versatile theoretical tool for sample characterization.

We would like to thank B. Jusserand and M. Cardona for useful discussions and the SERC LDS and Computational Science Initiatives and ESPRIT Basic Research Action No. 3043 for financial support for this project.

- \*New address: Department of Physics, The University of Newcastle upon Tyne, Newcastle upon Tyne NE1 7RU, United Kingdom.
- <sup>1</sup>B. Jusserand and D. Paquet, *Phys. Rev. Lett.* **56**, 1752 (1986).
- <sup>2</sup>B. Jusserand and M. Cardona, in *Light Scattering in Solids* (Springer-Verlag, Berlin, 1989), Vol. 5.
- <sup>3</sup>B. Jusserand, F. Alexandre, D. Paquet, and G. LeRoux, *Appl. Phys. Lett.* **47**, 301 (1985).
- <sup>4</sup>M. Nakayama, K. Kubota, H. Kato, S. Chika, and N. Sano, *Solid State Commun.* **53**, 493 (1985); A. Ishibashi, M. Habashi, Y. Mori, K. Kaneko, S. Kanado, and N. Watanabe, *Phys. Rev. B* **33**, 2887 (1986); M. Cardona, T. Suemoto, N. E. Christien, T. Isu, and K. Ploog, *ibid.* **36**, 5906 (1987); G. Fasol, M. Tanaka, H. Sakaki, and Y. Horikoshi, *ibid.* **38**, 6056 (1988).
- <sup>5</sup>G. Kanellis, *Phys. Rev. B* **35**, 746 (1987).
- <sup>6</sup>S. Baroni, P. Giannozzi, and E. Molinari, *Phys. Rev. B* **41**, 3870 (1990); E. Molinari, S. Baroni, P. Giannozzi, and S. de Gironcoli, in *Proceedings of the 20th International Conference on Physics of Semiconductors*, Thessaloniki, Greece, 1990, edited by E. Anastassakis and J. Joannopoulos (World-Scientific, Singapore, 1990), p. 1429.
- <sup>7</sup>A. B. Chen *Phys. Rev. B* **7**, 2230 (1973).
- <sup>8</sup>H. Eschrig, R. Richter, and B. Velicky, *J. Phys. C* **19**, 7173 (1986).
- <sup>9</sup>K. Kunc, M. Balkanski, and M. Nusimovici, *Phys. Status Solidi B* **72**, 229 (1975).
- <sup>10</sup>M. Tanaka, H. Ichinose, T. Furuta, Y. Ishida, and H. Sakaki, *J. Phys. (Paris) C* **5**, 101 (1985).
- <sup>11</sup>S. F. Ren, H. Chen, and Y.-C. Chang, *Phys. Rev. B* **37**, 8899 (1989).
- <sup>12</sup>W. Hayes, R. Springett, M. S. Skolnick, and C. R. Whitehouse (unpublished).
- <sup>13</sup>A. K. Sood, J. Menendez, M. Cardona, and K. Ploog, *Phys. Rev. Lett.* **54**, 2115 (1985).
- <sup>14</sup>B. Jusserand, F. Mollot, and D. Paquet, *Surf. Sci.* **228**, 151 (1990).